First Temperature and Velocity Measurements of the Dense Fuel Layer in Inertial Confinement Fusion Experiments

O. M. Mannion,[1] A. J. Crilly,[2] C. J. Forrest,[1] B. D. Appelbe,[2] Z. L. Mohamed,[1] V. Yu. Glebov,[1] V. Gopalaswamy,[1] V. N. Goncharov,[1] J. P. Knauer,[1] T. C. Sangster,[1] C. Stoeckl,[1] J. P. Chittenden,[2] and S. P. Regan[1]

[1]Laboratory for Laser Energetics, University of Rochester
[2]Centre for Inertial Fusion Studies, The Blackett Laboratory, Imperial College, London

The hydrodynamic properties of the shell in cryogenic inertial confinement fusion (ICF) experiments are of vital importance but have yet to be measured experimentally. Recent theoretical work[1] has demonstrated how the spectral shape of the kinematic edges in the neutron energy spectrum emitted from an ICF target could be used to infer the hydrodynamic properties of the dense DT fuel layer. When an incident neutron of energy $E_{n,i}$ elastically scatters off a stationary ion, the neutron will exit the scattering event at an energy $E_{n,f} = E_{n,i}\left[A^2 + 1 + 2A\cos(\theta_{cm})\right]/(A+1)^2$, where A is the ion-to-neutron mass ratio and θ_{cm} is the neutron scattering angle in the center-of-mass frame. The minimum energy at which a neutron can exit an elastic-scattering event is called the kinematic limit and occurs when the neutron undergoes a backscatter event ($\theta_{cm} = \pi$), resulting in an outgoing neutron at energy $E_{bs} = E_{n,i}(A-1)/(A+1)$. Since no neutron can reach energies lower than E_{bs} through a single elastic-scattering event, the neutron energy spectrum will have a sharp edge feature located at E_{bs}. This feature is referred to as the kinematic (or backscatter) edge.

The kinematic limit is shifted if the scattering ion is moving (see Fig. 1). The magnitude of this shift is dependent on the relative velocity between the ion and neutron.[1] When neutrons scatter off a population of ions with a given ion-velocity distribution, the resulting edge feature is the superposition of the kinematic edge produced from many neutron–ion scattering events. This results in the measured kinematic edge containing information on the ion-velocity distribution. In particular, the mean $\overline{v}$ of the ion-velocity distribution will cause an energy shift in the resulting edge location, while the variance Δ_v^2 of the ion-velocity distri-

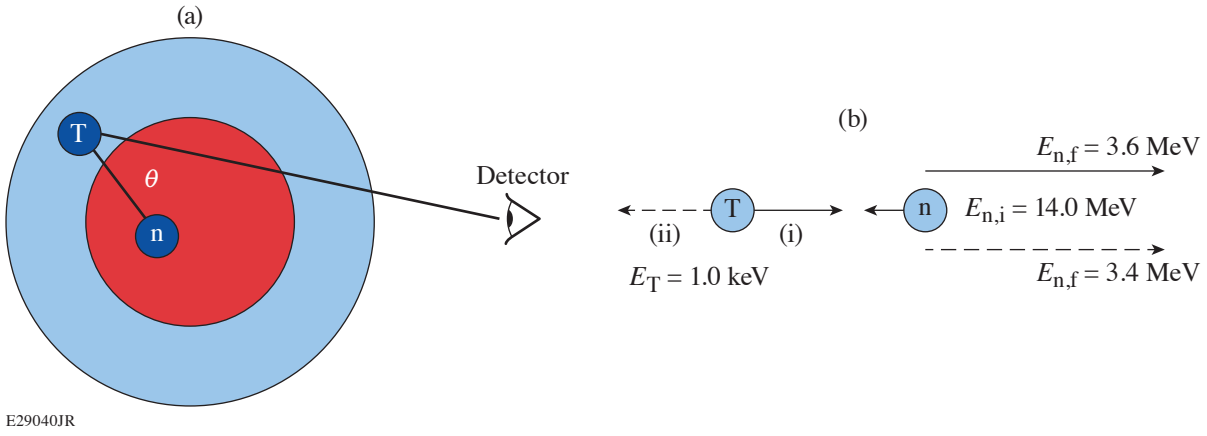

Figure 1
(a) A schematic of neutron scattering in a compressed ICF target, which consists of a low-density, high-temperature hot spot (red), surrounded by a low-temperature, high-density shell (blue). (b) Backscatter kinematics for a 1-keV triton moving (i) toward and (ii) away from an incident DT neutron.

bution will cause a change in the slope of the edge. Therefore, the spectral shape of the kinematic edge produced when neutrons scatter off a material can be used to diagnose the moments of the ion-velocity distribution within the material.

Neutron scattering occurs throughout the compressed ICF target, which results in the kinematic edges sampling the ion-velocity distributions in many regions of the capsule. The ion-velocity distribution being measured by the kinematic edges from an ICF target is the scatter-weighted, ion-velocity distribution. The shape of this distribution has been studied[1] using the 1-D radiation-hydrodynamic code *LILAC* and found to be well described by a normal distribution with a mean $\overline{v}$ and variance Δ_v^2. The mean $\overline{v}$ is the scatter-weighted velocity of the shell, while the variance Δ_v^2 is related to the scatter-weighted temperature and velocity variance of the shell.

The nT kinematic edge has been measured for an ensemble of direct-drive DT cryogenic implosions on OMEGA using a neutron time-of-flight (nTOF) detector, and a forward-fit analysis has been applied to infer the moments of the triton velocity distribution. Example nT-edge measurements along with the forward fit are shown in Fig. 2. To minimize the effect of implosion asymmetries on the nT-edge measurements, only experiments with apparent ion temperature asymmetry <1.0 keV and hot-spot flow velocities <80 km/s were considered.

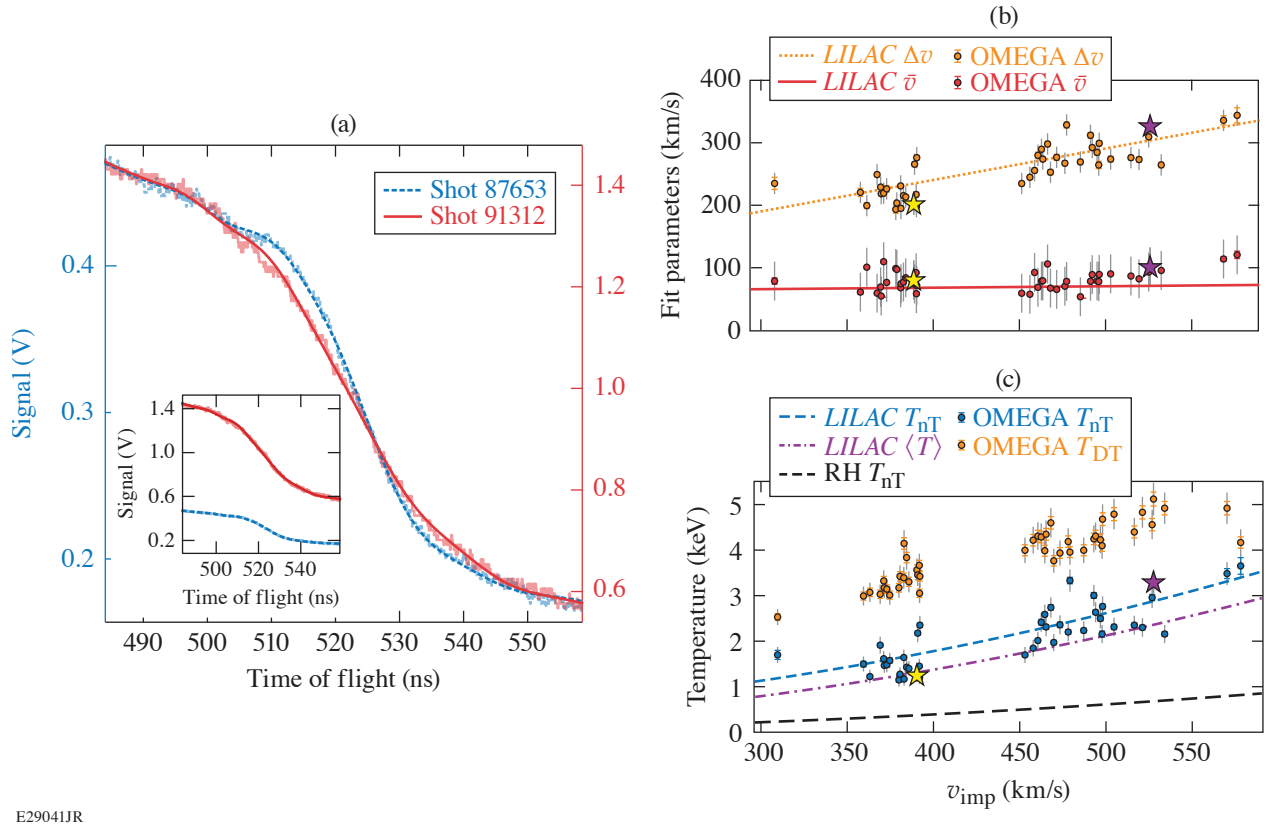

Figure 2
(a) The measured nTOF signal (shaded) and forward fit (solid and dashed lines) in the nT-edge region for two experiments. The primary DT neutron yields and areal density for these two experiments were different, resulting in the measured nT edges having different amplitudes. The data have been plotted as two separate signal axes to facilitate comparison of the nT spectral shape. The inset shows the nTOF signals plotted on the same signal axis for reference. (b) The measured (circles) and *LILAC* calculated (lines) values for Δv and $\overline{v}$ as functions of calculated implosion velocity. (c) The measured nT edge (blue circles) and primary DT (orange circles) temperatures as functions of implosion velocity. Also shown are the *LILAC*-inferred temperature from the nT edge (blue dashed line), the *LILAC* scatter-averaged triton temperature (purple dashed–dotted line), and the temperature of the shocked material as calculated by strong shock Rankine–Hugoniot (RH) conditions (black dashed line). The statistical uncertainties are shown as error bars on the points and the systematic uncertainties are shown as gray bars on the points. The results for the experiments in (a) are indicated as stars for shots 87653 (yellow) and 91312 (purple).

The inferred $\overline{v}$ and Δ_v^2 values from the ensemble of experiments are shown in Fig. 2 as a function of the implosion velocity v_{imp} as calculated by *LILAC*. Calculations of Δ_v^2 and $\overline{v}$ from post-shot *LILAC* simulations are in good agreement with the measured values. The inferred shell velocities $\overline{v}$ are uniform across the experiments on OMEGA with an average velocity of 79 km/s and standard deviation of 16 km/s. The measured velocities are small in comparison to the implosion velocity due to the measurement sampling the shell velocity near peak compression [see Fig. 2(b)]. The $\overline{v}$ measurements indicate there is little variability in the shell residual kinetic energy for these implosions, which is expected since these implosions were chosen for their symmetry.

The nT- and DT-inferred temperatures are shown in Fig. 2(c) as functions of implosion velocity. The nT measured temperatures are lower than the DT temperatures. This is a result of the DT-inferred temperature being a neutron-averaged quantity, which results in the inferred value being weighted toward the region in which fusion reactions are occurring (i.e., the hot spot), whereas the nT-inferred temperature is a scatter-averaged quantity, which results in the inferred value being weighted toward the denser and colder regions (i.e., the shell). The increase in the nT-edge temperature with implosion velocity is due to an increase of the thermal conduction from the hot spot into the shell. The thermal conduction of a fully ionized ideal gas[2] has a temperature dependence of $T^{5/2}$. The higher initial hot-spot temperatures achieved with higher implosion velocities [see Fig. 2(b)] result in an increased thermal conduction of heat from the hot spot into the shell. This increases the temperature of the shell while also increasing the ablation rate of cold material into the hot spot. Consequently, the fraction of neutron scattering in shocked material >1 keV increases linearly with implosion velocity while the contribution from material <1 keV decreases. Since the nT edge temperature is scatter weighted, the increasing contribution from material >1 keV is the dominant contribution to the increased nT inferred temperature.

The temperature and velocity measurements presented here, along with areal-density measurements of the shell, now provide a complete set of hydrodynamic properties of the dense fuel layer near peak compression. The temperature measurements provide a key piece of information required to measure the shell adiabat in cryogenic ICF experiment. The shell-velocity measurements provide the first experimental evidence of residual motion of the shell near peak compression and provide the first insights into the conversion efficiency of shell kinetic energy to thermal energy of the hot spot. Future work will extend this analysis to multiple lines of sight and investigate asymmetric implosions. Additionally, this technique can be applied to other backscatter edges that occur in ICF experiments such as the deuterium backscatter edge at 1.5 MeV in DT cryogenic implosions or the beryllium edge that exists in magnetized liner fusion experiments. Finally, this technique can be applied to a more general set of high-energy-density experiments that require measurements of the hydrodynamic properties of dense shocked materials.

This material is based upon work supported by the Department of Energy National Nuclear Security Administration under Award Number DE-NA0003856, the University of Rochester, and the New York State Energy Research and Development Authority.

1. A. J. Crilly *et al.*, Phys. Plasmas **27**, 012701 (2020).

2. L. Spitzer, *Physics of Fully Ionized Gases*, 2nd rev. ed., Interscience Tracts on Physics and Astronomy (Wiley Interscience, New York, 1962).